

An exciting application of piecewise-linear holistic discretisation

G. A. Jarrad A. J. Roberts*

Thursday 1st October, 2015

Abstract



The fidelity of numerical simulation of a spatio-temporal dynamical system is largely constrained by the chosen discretisation of the PDE. In particular, the modeller is typically free to choose arbitrary finite-element forms for the various spatial derivatives, without necessarily having knowledge of the accuracy of the resulting numerical schemes. The holistic discretisation approach described in this paper obviates the problem of arbitration.

Centre manifold theory is applied to derive an asymptotically accurate representation of the microscale dynamics of the one-dimensional Burgers' equation. In the process, the corresponding macroscale dynamics are constrained to match the microscale solution at discrete grid-points. The resulting representation of macroscale evolution provides an unambiguous discretisation of the PDE, suitable for numerical simulation.

The iterative process starts with a choice of the leading, macroscale approximation to the linearised system. Suitable internal boundary conditions are then induced on the spatial derivatives at the end-points of each discrete interval. Although the choice of IBCs might appear to be arbitrary, they are in fact governed by the placement of the grid-points and the form of the leading discrete approximation. The particular approach taken here is to start with a piecewise linear but continuous approximation, in contrast to similar analyses that use piecewise constant, discontinuous approximations. This is motivated by the principle that a more accurate leading approximation should lead to faster convergence of the asymptotic solution, via the Rayleigh-Ritz theorem.

*School of Mathematical Sciences, University of Adelaide, South Australia 5005, Australia. <mailto:anthony.roberts@adelaide.edu.au>

Further iterations of the centre manifold process lead inexorably to a temporal evolution formulation of the macroscale dynamics, holistically informed by the underlying microscale dynamics. We examine the accuracy and stability of the resulting numerical scheme, in comparison to the behaviours of several other typical approximations.

1 Introduction

This article’s scope is the accurate spatial discretisation of nonlinear PDEs for a field $u(x, t)$ satisfying reaction-advection-diffusion PDEs in the general form

$$u_t = F(u_x)_x + \alpha G(x, u, u_x) \quad (1)$$

where subscripts x and t denote spatial and temporal derivatives, respectively, and for suitably smooth functions F and G . Given $N+1$ discrete points in space, $x = X_j$ for $j = 0, \dots, N$, we define grid values $U_j(t) = u(X_j, t)$. Then the aims are to: firstly, establish that in principle there exists an *exact* closure of the dynamics of the PDE (1) in terms of these grid values, $d\vec{U}/dt = \vec{g}(\vec{U})$; secondly, establish that such a closure is emergent from general initial conditions; thirdly, show how to construct systematic approximations to the in-principle closure; and fourthly, evaluate its performance for the classic example of the nonlinear advection–diffusion Burgers’ PDE

$$\frac{\partial u}{\partial t} = \nu \frac{\partial^2 u}{\partial x^2} - \alpha u \frac{\partial u}{\partial x}. \quad (2)$$

Generalisation of the approach to two or more spatial dimensions remains for further research.

The spatial domain \mathbb{X} is of length L , $0 \leq x \leq L$, and we mostly restrict attention to solutions $u(x, t)$ which are L -periodic in space, but occasionally comment on the cases of Dirichlet boundary conditions, $u(0, t) = u(L, t) = 0$, and Neumann boundary conditions, $u_x(0, t) = u_x(L, t) = 0$. The first step is to partition \mathbb{X} into N equi-spaced intervals bounded by the $N+1$ grid-points X_j with spacing H . Traditional spatial discretisation of such PDEs, whether finite difference, finite element, or finite volume, imposes assumed fields in each element and then derives approximate rules for the evolution in time of the parameters of the imposed fit.

Our approach is to let the PDE (2) determine the subgrid structures in order to remain faithful to the PDE. Let the dynamics of the field $u(x, t)$ be summarised by the coarse variables $\vec{U} = (U_1, U_2, \dots, U_N)$, where these are grid values

$$U_j(t) := u(X_j, t) \text{ for all } t \in \mathbb{T}. \quad (3)$$

Theory to be discussed asserts that in principle an *exact* closure exists: that is, there is some coarse temporal evolution

$$\dot{U}_j = g_j(\vec{U}) \quad \text{for all } j \quad (4)$$

that gives exact solutions of the PDE. A traditional approach is to use centred approximations:

$$\begin{aligned} \dot{U}_j &\approx -\alpha \frac{1}{2H} U_j (U_{j+1} - U_{j-1}) + \nu \frac{1}{H^2} (U_{j+1} - 2U_j + U_{j-1}) \\ &= -\alpha U_j \mu \delta U_j / H + \nu \delta^2 U_j / H^2, \end{aligned}$$

for centred difference $\delta = \sigma^{1/2} - \sigma^{-1/2}$, centred mean $\mu = (\sigma^{1/2} + \sigma^{-1/2})/2$, and shift operator $\sigma U_j = U_{j+1}$. However, the nonlinear advection term has another plausible representation, namely the conservative form $\mu \delta(U_j^2)/2H$. For illustrative purposes, section ?? compares results with those of a convex combination of these two representations; that is, section ?? compares results with Burgers' PDE (2) discretised to the so-called mixture model

$$\dot{U}_j = -(1 - \theta) \alpha \frac{U_j \mu \delta U_j}{H} - \theta \alpha \frac{\mu \delta(U_j^2)}{2H} + \nu \frac{\delta^2 U_j}{H^2}. \quad (5)$$

In contrast, Section 4 shows our holistic approach has no such representational ambiguity, and constructs at first-order the specific model

$$\dot{U}_j = S \left[-\alpha \frac{U_j \mu \delta U_j}{3H} - \alpha \frac{\mu \delta(U_j^2)}{3H} + \nu \frac{\delta^2 U_j}{H^2} \right], \quad (6)$$

for nonlocal operator $S = (1 + \delta^2/6)^{-1}$. Apart from the operator S , this holistic model matches the mixture model (5) for parameter $\theta = \frac{2}{3}$. This parameter value is exactly the critical value predicted by Fornberg (1973) to be necessary for stable simulation (with $\nu = 0$ and $\alpha = 1$) for a selection of numerical integration schemes. Section 5 further compares the numerical behaviour of the holistic and mixture models.

The final part of the process is to express the physical field $u(x, t)$ in terms of the coarse variables $\vec{U}(t)$. That is, as illustrated by the two approximate examples of Figure 1, we construct the field

$$u(x, t) = u(x, \vec{U}(t)), \quad (7)$$

where the time evolution of u comes via the evolving coarse variables $\vec{U}(t)$. Whether the symbol u denotes $u(x, t)$ or $u(x, \vec{U})$ should be clear from the context. The complete holistic framework comprises equations (4) and (7),

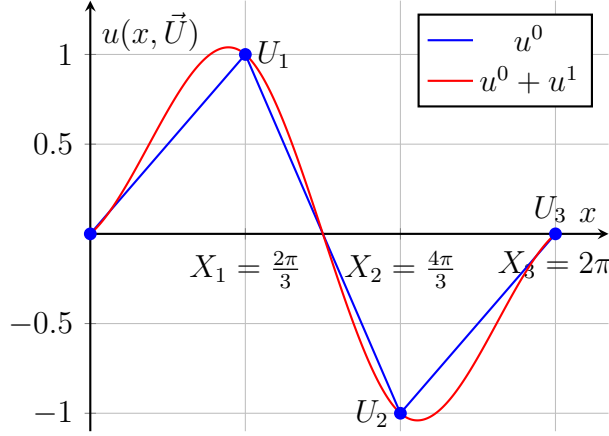


Figure 1: An example of the smooth subgrid field provided by the holistic discretisation process, where the piecewise-linear initial approximation $u^0(x, \vec{U})$ is smoothed by the first-order correction $u^1(x, \vec{U})$ (for nonlinearity $\alpha = 0$). The correction u^1 forms a cubic spline; however, it is derived directly from the PDE itself, rather than obtained by imposing such an interpolation.

along with the addition of suitable boundary conditions that are discussed in Section 3.

The Rayleigh–Ritz theorem motivates our choice for a leading approximation that is a piecewise linear function (e.g., the blue u^1 of Figure 1), in contrast to the usual piecewise constant one (Roberts 2001, 2003, Roberts et al. 2014). Approximately constructing a centre manifold is analogous to estimating eigenvalues of a perturbed matrix. For a self-adjoint operator \mathcal{L} , the Rayleigh–Ritz theorem is that an approximate eigenvector \vec{v} , with error $\mathcal{O}(\epsilon)$, predicts a corresponding eigenvalue $\lambda = \langle \vec{v}, \mathcal{L}\vec{v} \rangle / \|\vec{v}\|^2$ with asymptotically smaller error $\mathcal{O}(\epsilon^2)$. This suggests that the more accurate we make an initial approximation to the field u , the more accurate the predicted evolution on the slow manifold. Consequently, this article develops a systematic approximation to an in-principle exact discrete closure based upon systematically refining a piecewise linear and continuous subspace approximation to the field u .

2 An example introduces theory and method

As an introduction to the methodology, this section investigates the modelling of Burgers’ PDE (2) on the specific domain $-1 < x < 1$, with basic Dirichlet boundary conditions that $u(\pm 1, t) = 0$, and with viscosity $\nu = 1$

for definiteness. For introductory simplicity, the domain space is partitioned into just two intervals, $-1 < x < 0$ and $0 < x < 1$, by the interior ‘grid point’ $X = 0$. Our aim is to model the dynamics of the whole field $u(x, t)$ by simply the dynamics of the ‘grid value’ $U(t) := u(0, t)$ of the field at this central grid point.

The dynamics in the two intervals need to be coupled to each other to form a solution valid over the whole domain. Conventional numerical methods *impose* an assumed interpolation field and then derive a corresponding model. In contrast, here we craft a coupling that moderates the communication between the two intervals, and then lets the PDE (2) itself tell us the appropriate fields and model. The desired full coupling between the two intervals is of C^1 continuity: $[u] = [u_x] = 0$ where we introduce $[\cdot]$ to denote the jump in value across the grid point $X = 0$; that is, $[u] = u|_{0+} - u|_{0-}$. For reasons developed below, we embed Burgers’ PDE (2) in a family of problems with the moderated coupling between intervals of

$$[u] = 0 \quad \text{and} \quad [u_x] + 2(1 - \gamma)u = 0 \quad \text{at } x = X = 0; \quad (8)$$

that is, the field is continuous but the derivative has a discontinuity depending upon homotopy parameter γ (corresponding to the general case (12)). We derive below that $\gamma = 0$ provides a useful base to apply powerful centre manifold theory. When $\gamma = 1$, the coupling (8) reverts to requiring C^1 continuity across $x = 0$ to restore the PDE over the entire spatial domain.

To show there is a useful (slow) centre manifold, we start with equilibria in the system (corresponding to Lemma 1). The PDE (2), with diffusivity $\nu = 1$, together with coupling conditions (8), and the Dirichlet boundary conditions, has a subspace \mathbb{E} of equilibria: for each U ,

$$u = (1 - |x|)U \quad \text{and} \quad \gamma = \alpha = 0. \quad (9)$$

The spectrum about each of these equilibria determine the manifold structure (corresponding to Lemmas 3 and 4). We seek linearised solutions $u(x, t) \approx (1 - |x|)U + e^{\lambda t}v(x)$ for small v : the diffusion PDE (2) becomes the eigenproblem

$$-v_{xx} + \lambda v = 0, \quad \text{such that } [v] = [v_x] + 2v = 0 \text{ at } x = 0, \quad (10)$$

with homogeneous Dirichlet boundary conditions $v(\pm 1) = 0$.

- Corresponding to eigenvalue $\lambda = 0$ is the neutral solution $v \propto 1 - |x|$ reflecting the direction of the subspace \mathbb{E} of equilibria.

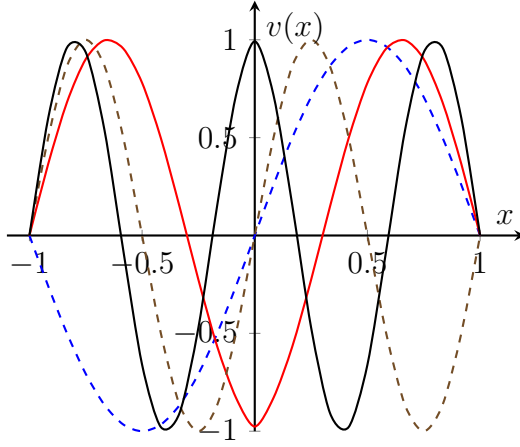


Figure 2: Eigenfunctions $v(x)$ of the linearised problem (10) corresponding to negative eigenvalues: blue dashed, $-\pi^2$; red solid, -20.191 ; brown dashed, $-4\pi^2$; and black solid, -59.680 .

- Negative eigenvalues $\lambda = -k^2$ arise corresponding to eigenfunctions of the form $v \propto \sin[k(1 - |x|)]$ which arises by necessity from the PDE, the homogeneous Dirichlet boundary conditions, and the continuity of v . By straightforward algebra, the jump in the derivative determines the wavenumbers k from the solutions of $k = \tan k$, namely the wavenumbers $k = 4.4934, 7.7253, 10.9041, \dots$. That is, non-zero eigenvalues of the linearised problem are $\lambda = -20.191, -59.680, -118.900, \dots$. Figure 2 plots (solid) the corresponding eigenfunctions for the two smallest magnitude of these eigenvalues.
- Negative eigenvalues also arise from eigenfunctions of the form $v \propto \sin(kx)$. The boundary and coupling conditions determine the wavenumbers $k = n\pi$ for $n = 1, 2, 3, \dots$. That is, the other non-zero eigenvalues are $\lambda = -\pi^2, -4\pi^2, -9\pi^2, \dots$. Figure 2 plots (dashed) the corresponding eigenfunctions for the two smallest magnitude of these eigenvalues.

One of the beautiful properties of the coupling conditions (8) is that with them the diffusion operator $\partial^2/\partial x^2$ is self-adjoint (analogous to Lemma 2). Hence there are only real eigenvalues of the linear problem (10), namely the ones found above. To confirm self-adjointness under the usual inner product, $\langle u, v \rangle = \int_{-1}^1 u(x)v(x) dx$, consider

$$\begin{aligned}
 \langle u, v_{xx} \rangle &= \int_{-1}^1 uv_{xx} dx \quad (\text{then using integration by parts}) \\
 &= [uv_x - vu_x]_{-1}^{0^-} + [uv_x - vu_x]_{0^+}^1 + \int_{-1}^1 u_{xx}v dx \\
 &\quad (\text{using the Dirichlet boundary conditions})
 \end{aligned}$$

$$\begin{aligned}
&= -[uv_x - vu_x]_{0^-}^{0^+} + \langle u_{xx}, v \rangle \\
&\quad \text{(using continuity at } x = 0\text{)} \\
&= -u|_0[v_x] + v|_0[u_x] + \langle u_{xx}, v \rangle \\
&\quad \text{(using the jump in derivative at } x = 0\text{)} \\
&= u|_0 2(1 - \gamma)v|_0 - v|_0 2(1 - \gamma)u|_0 + \langle u_{xx}, v \rangle \\
&= \langle u_{xx}, v \rangle.
\end{aligned}$$

This useful self-adjointness is not a property of previous holistic discretisations (Roberts 2014, Part V, e.g.), but is a new feature maintained for the approach of this article.

Because the spectrum consists of a zero eigenvalue and all the rest negative ($\leq -\pi^2 < -9$), centre manifold theory (Carr 1981, e.g.) assures us that there exists a slow manifold in some neighbourhood of the subspace \mathbb{E} of equilibria (corresponding to Theorem 5): that is, global in amplitude U and local in parameters γ and α . Also, the theory guarantees that all solutions in the neighbourhood are attracted exponentially quickly, at least as fast as roughly e^{-9t} , to solutions on the slow manifold. That is, the slow manifold and the evolution thereon emerges from general initial conditions.

A theorem (Carr 1981, Thm. 6.10, e.g.) also guarantees that when we approximate the slow manifold and its evolution to a residual of $\mathcal{O}(\gamma^p)$, the slow manifold and its evolution are correct to errors $\mathcal{O}(\gamma^p)$. By straightforward machinations not detailed here (Roberts 1997, 2014, Ch. 14) we arrive at the expressions that the slow manifold and the evolution thereon are

$$u \approx [1 - |x| + \gamma(|x| - \tfrac{3}{2}x^2 + \tfrac{1}{2}|x|^3)] U \quad \text{such that } \dot{U} \approx -3\gamma U. \quad (11)$$

Substituting these expressions into the heat PDE (2) ($\alpha = 0$), and the boundary and coupling conditions (8) we find the equations are satisfied to residual $\mathcal{O}(\gamma^2)$ and so the approximation theorem asserts these expressions are approximations with errors $\mathcal{O}(\gamma^2)$.

Although this approximation is based around parameter $\gamma = 0$, we are interested in the physical value of the parameter $\gamma = 1$. Evaluating the slow manifold (11) at $\gamma = 1$ gives

$$u \approx (1 - \tfrac{3}{2}x^2 + \tfrac{1}{2}|x|^3)U \quad \text{such that } \dot{U} \approx -3U.$$

The field u , plotted in Figure 3, is an excellent cubic spline approximation to the correct $U \cos(\pi x/2)$ eigenfunction, also plotted in Figure 3. The predicted evolution $U \propto e^{-3t}$ is a good approximation to the correct decay rate of $-\pi^2/4$.

One key question is how can we be sure that evaluating at finite $\gamma = 1$ is within the finite neighbourhood of validity of the slow manifold? Here

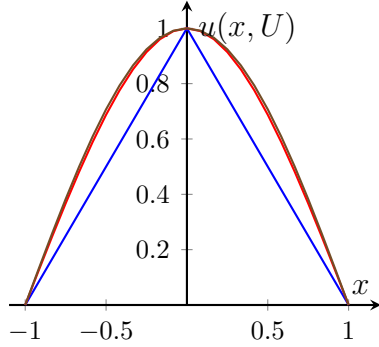


Figure 3: A comparison of approximations to the long-term, quasi-stationary, decay of the heat PDE: blue, $u \propto 1 - |x|$ is the basic linear approximation (13); red, the derived cubic spline (11) at full coupling $\gamma = 1$; and, almost indistinguishable, brown, is the exact mode $u \propto \cos(\pi x/2)$.

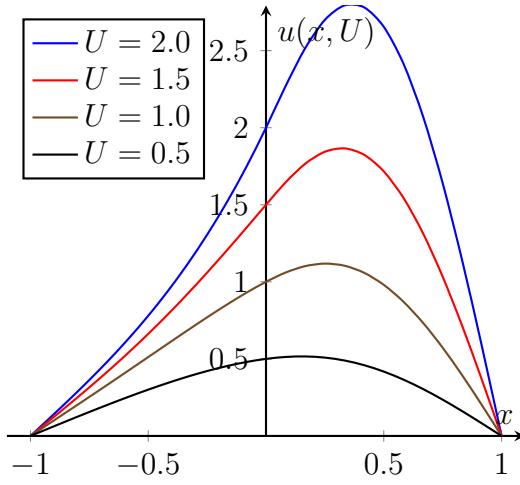


Figure 4: Nonlinear slow manifold for Burgers' PDE (2) for viscosity $\nu = 1$ and nonlinearity $\alpha = 2$. Drawn is the slow manifold $u(x, U)$ for representative amplitudes $U = \frac{1}{2}, 1, \frac{3}{2}, 2$ to show the larger deformation at larger amplitudes. This approximation to the slow manifold was computed to errors $\mathcal{O}(\gamma^3 + \alpha^3)$ and evaluated at full coupling $\gamma = 1$.

computer algebra (Roberts 1997, 2014, Ch. 14) straightforwardly computes to high order to determine, for example, the slow evolution

$$\dot{U} = -[3\gamma - 0.6\gamma^2 + 0.06857\gamma^3 - 0.00128\gamma^5 + 0.00008\gamma^6 + 0.00004\gamma^7 + \mathcal{O}(\gamma^8)]U.$$

Evidently the series in γ appears to have a radius of convergence much larger than one¹. Hence, we predict that the neighbourhood of validity around \mathbb{E} includes the case of interest, $\gamma = 1$.

Centre manifold theory (Carr 1981, Roberts 2014, Ch. 4, e.g.) was designed for nonlinear problems. Thus it also applies here to the nonlinear Burgers' PDE (2) now with nonlinearity parametrised by α and similarly modelled with two intervals on the domain $-1 < x < 1$. For example, modified computer algebra (Roberts 1997, 2014, Ch. 14) constructs the slow

¹Construction of the slow manifold to 40th order in γ (for $\alpha = 0$) followed by a generalised Domb–Sykes plot (Mercer & Roberts 1990, Appendix) predicts convergence for all $|\gamma| < 3.8$ —the convergence limiting singularity lying at an angle 103° to the real γ -axis.

manifold plotted in Figure 4 on which the nonlinear evolution is

$$\dot{U} = -(3\gamma + \frac{3}{5}\gamma^2)U - \frac{1}{15}\gamma^2\alpha^2U^3 + \mathcal{O}(\gamma^3 + \alpha^3).$$

The nonlinear advection of Burgers' PDE generates steeper gradients (Figure 4) that enhance the decay as expressed by the cubic nonlinearity in this evolution equation for amplitude $U(t)$.

Key properties of this example are also exhibited in the application of the approach to the more general spatial discretisations discussed in subsequent sections: an analogous inter-element coupling engenders an emergent slow manifold; the linearised operator is self-adjoint; the first iteration constructs a cubic spline; and the resultant model at full coupling has attractive properties.

3 Linearisation establishes the existence of a closure

We use centre manifold theory (Carr 1981, Haragus & Iooss 2011, e.g.) to establish (Theorem 5) the in-principle existence and emergence of an exact closure to the dynamics of PDEs in the class (1). Centre manifold theory is based upon an equilibrium or subspace of equilibria, and follows primarily from the spectrum of the linearised dynamics (Roberts 2014, e.g.).

To find useful equilibria we embed the PDE (1) in a wider class of problems. First partition the spatial domain into the N intervals between the grid points $x = X_j$: let the interval $\mathbb{X}_j = \{x \mid X_{j-1} < x < X_j\}$ and denote the punctured domain $\tilde{\mathbb{X}} := \mathbb{X} \setminus \{X_0, X_1, \dots, X_N\}$. For definiteness take the boundary conditions on the field $u(x, t)$ to be that it is L -periodic in space. Then use $u_j(x, t)$ to denote solutions of the PDE (1) on the interval \mathbb{X}_j , and reserve $u(x, t)$, over \mathbb{X} or $\tilde{\mathbb{X}}$ as appropriate, to denote the union over all intervals of such solutions. To restore the original PDE (1) over the whole domain \mathbb{X} we couple the fields on each interval together. By controlling the information flow between intervals, we embed the original PDE over the whole domain to a useful base problem. The general coupling conditions are

$$[u]_j = u|_{X_j^+} - u|_{X_j^-} = 0 \quad \text{and} \quad (12a)$$

$$[\nu u_x]_j = \frac{C(\gamma)}{H} \left[(\nu u)|_{X_{j+1}^-} - (\nu u)|_{X_j^+} + (\nu u)|_{X_{j-1}^+} - (\nu u)|_{X_j^-} \right], \quad (12b)$$

where coefficient $\nu(x) = F'(u_x)$ is the effective diffusivity at each point in $\tilde{\mathbb{X}}$, via the gradient u_x , and where the factor $C(\gamma)$ is some smooth function such that $C(0) = 1$ and $C(1) = 0$ (typically $C(\gamma) := 1 - \gamma$).

Lemma 1 (equilibria). *The PDE (1) on domain $\tilde{\mathbb{X}}$ with coupling conditions (12) possesses an N -dimensional subspace \mathbb{E} of equilibria, parametrised by $\vec{U} = (U_1, U_2, \dots, U_N)$, for parameters $\alpha = \gamma = 0$ of piecewise linear solutions $u^*(x)$ such that on the j th interval the field*

$$u_j^*(x) = (1 - \xi_j)U_{j-1} + \xi_j U_j \quad \text{where } \xi_j = (x - X_{j-1})/H \quad (13)$$

is a local scaled space variable.

Proof. With nonlinearity $\alpha = 0$ the PDE (1) takes the form $u_t = F(u_x)_x$. For the piecewise linear field (13), the gradient $u_x^* = (U_j - U_{j-1})/H$ is constant on each \mathbb{X}_j . Hence $F(u_x^*)$ is constant on each \mathbb{X}_j . Consequently, $F(u_x^*)_x = 0$ on $\tilde{\mathbb{X}}$, giving an equilibria of the PDE on $\tilde{\mathbb{X}}$.

From the field (13), $u_j^*(X_j^-) = U_j = u_{j+1}^*(X_j^+)$ and hence $u^*(x)$ is continuous at X_j to satisfy the coupling condition (12a).

Lastly, consider the condition (12b) on the jump in the derivative. For the field (13), the gradient is $u_x^* = (U_j - U_{j-1})/H$ so, in terms of the constants

$$\nu_j := F'(u_{jx}^*) = F'\left(\frac{U_j - U_{j-1}}{H}\right), \quad (14)$$

the jump in gradient is

$$\begin{aligned} [\nu u_x^*]_j &= \nu_{j+1} \frac{U_{j+1} - U_j}{H} - \nu_j \frac{U_j - U_{j-1}}{H} \\ &= \frac{1}{H} (\nu_{j+1} U_{j+1} - \nu_{j+1} U_j + \nu_j U_{j-1} - \nu_j U_j) \\ &= \frac{1}{H} \left(\nu|_{X_{j+1}^-} u^*|_{X_{j+1}^-} - \nu|_{X_j^+} u^*|_{X_j^+} + \nu|_{X_{j-1}^+} u^*|_{X_{j-1}^+} - \nu|_{X_j^-} u^*|_{X_j^-} \right), \end{aligned}$$

which is the required right-hand side of (12b) for coupling parameter $\gamma = 0$ (as $C(0) = 1$). Hence, the piecewise linear fields (13), with $\alpha = \gamma = 0$, are equilibria for all \vec{U} , and clearly form an N -D subspace. \square

The spectrum comes from the linearised dynamics around each of the equilibria \mathbb{E} . Seek solutions $u = u^*(x) + \hat{u}(x, t)$ of the general PDE (1) where $\hat{u}(x, t)$ denotes a small perturbation to the equilibrium (13). Use $\hat{u}_j(x, t)$ as a synonym for $\hat{u}(x, t)$ on the j th interval \mathbb{X}_j . Then for parameters $\alpha = \gamma = 0$ and small \hat{u} , the PDE (1) linearises to

$$\hat{u}_t = F'(u_x^*)\hat{u}_{xx} = \nu(x)\hat{u}_{xx} \quad \text{on } \tilde{\mathbb{X}}; \quad \text{that is, } \hat{u}_{jt} = \nu_j \hat{u}_{jxx} \quad \text{on } \mathbb{X}_j. \quad (15a)$$

The coupling conditions (12) are linear, so they are $[\hat{u}]_j = 0$ and $[\nu \hat{u}_x]_j = \frac{1}{H} [(\nu \hat{u})|_{X_{j+1}^-} - (\nu \hat{u})|_{X_j^+} + (\nu \hat{u})|_{X_{j-1}^+} - (\nu \hat{u})|_{X_j^-}]$; that is,

$$\hat{u}_{j+1}(X_j) = \hat{u}_j(X_j) \quad \text{and} \quad (15b)$$

$$\begin{aligned}
& \nu_{j+1} \hat{u}_{j+1,x}(X_j) - \nu_j \hat{u}_{jx}(X_j) \\
&= \frac{1}{H} [\nu_{j+1} \hat{u}_{j+1}(X_{j+1}) - \nu_{j+1} \hat{u}_{j+1}(X_j) + \nu_j \hat{u}_j(X_{j-1}) - \nu_j \hat{u}_j(X_j)]. \quad (15c)
\end{aligned}$$

The next lemma certifies that this linearised system is self-adjoint and so we need only seek real eigenvalues in the spectrum.

Lemma 2 (self-adjoint). *The differential operator appearing in (15), namely $\mathcal{L} = \nu \partial^2 / \partial x^2$ on $\tilde{\mathbb{X}}$ subject to (15b)–(15c) and for L -periodic solutions, is self-adjoint upon using the usual inner product $\langle v, u \rangle := \int_{\tilde{\mathbb{X}}} v u \, dx$.*

Proof. Straightforwardly use integration by parts (remembering that ν is piecewise constant):

$$\begin{aligned}
\langle v, \mathcal{L}u \rangle &= \int_{\tilde{\mathbb{X}}} v \nu u_{xx} \, dx \\
&= \sum_j [\nu v u_x - \nu u v_x]_{X_{j-1}^+}^{X_j^-} + \int_{\tilde{\mathbb{X}}} \nu v_{xx} u \, dx \\
&= \sum_j [\nu_j v_j(X_j^-) u_{jx}(X_j^-) - \nu_j u_j(X_j^-) v_{jx}(X_j^-) \\
&\quad - \nu_j v_j(X_{j-1}^+) u_{jx}(X_{j-1}^+) + \nu_j u_j(X_{j-1}^+) v_{jx}(X_{j-1}^+)] + \langle \mathcal{L}v, u \rangle \\
&\quad \text{(using the continuity (15b) and } U_j := u(X_j^\pm), V_j := v(X_j^\pm)) \\
&= \sum_j [\nu_j V_j u_{jx}(X_j^-) - \nu_j U_j v_{jx}(X_j^-) \\
&\quad - \nu_j V_{j-1} u_{jx}(X_{j-1}^+) + \nu_j U_{j-1} v_{jx}(X_{j-1}^+)] + \langle \mathcal{L}v, u \rangle \\
&\quad \text{(reindexing the last two terms in the sum, } j \mapsto j+1) \\
&= \sum_j [V_j \nu_j u_{jx}(X_j^-) - U_j \nu_j v_{jx}(X_j^-) \\
&\quad - V_j \nu_{j+1} u_{j+1,x}(X_j^+) + U_j \nu_{j+1} v_{j+1,x}(X_j^+)] + \langle \mathcal{L}v, u \rangle \\
&\quad \text{(replacing two pairs of terms via coupling (15c))} \\
&= \sum_j \left\{ -V_j \frac{1}{H} [\nu_{j+1} U_{j+1} - \nu_{j+1} U_j + \nu_j U_{j-1} - \nu_j U_j] \right. \\
&\quad \left. + U_j \frac{1}{H} [\nu_{j+1} V_{j+1} - \nu_{j+1} V_j + \nu_j V_{j-1} - \nu_j V_j] \right\} + \langle \mathcal{L}v, u \rangle \\
&\quad \text{(cancelling all terms in } U_j V_j) \\
&= \sum_j \frac{1}{H} \{-V_j \nu_{j+1} U_{j+1} - V_j \nu_j U_{j-1} + U_j \nu_{j+1} V_{j+1} + U_j \nu_j V_{j-1}\} \\
&\quad + \langle \mathcal{L}v, u \rangle \\
&\quad \text{(reindexing 2nd and 4th terms in the sum, } j \mapsto j+1)
\end{aligned}$$

$$= \sum_j 0 + \langle \mathcal{L}v, u \rangle = \langle \mathcal{L}v, u \rangle.$$

Hence, as required, the linear operator in the linearised system (15) is self-adjoint. It can be shown that self-adjointness also holds for Dirichlet and Neumann boundary conditions. \square

We turn to determining the spectrum of the general linearised system (15): first, the zero eigenvalues; and second, the non-zero eigenvalues. Because of the N -D subspace of equilibria \mathbb{E} , the linearised system must have N eigenvalues of zero. Corresponding basis eigenfunctions may be chosen to be

$$\phi_j(x) = \max(0, 1 - |x - X_j|/H)$$

so the equilibria (13) may be written $u^* = \sum_j \phi_j(x)U_j$. The localised triangular shape of these basis functions, incidentally, many will recognise as the fundamental “shape function” often invoked in the finite element method (O’Leary 2008, Strang & Fix 2008, e.g.). For the linearised PDE (15a) any eigenfunction corresponding to an eigenvalue of zero must be linear on each \mathbb{X}_j , and the continuity (15b) then guarantees there are no other eigenfunctions than those identified. By self-adjointness, there are no generalised eigenfunctions. Thus the slow subspace of the system (15) is N -D, namely \mathbb{E} .

For rigorous theory we notionally adjoin the two trivial dynamical equations $\alpha_t = \gamma_t = 0$ to the linearised system (15). Then, as $\alpha = \gamma = 0$, the equilibria (13) are $(0, 0, u^*(x))$. Thus strictly there are two extra zero eigenvalues associated with the trivial $\alpha_t = \gamma_t = 0$, and the corresponding slow subspace of each equilibria is $(N + 2)$ -D. Except for issues associated with the domain of validity, for simplicity we do not explicitly include these two trivial dynamical equations nor their eigenvalues in the following, but consider them implicit.

Lemma 3 (exponential dichotomy). *Provided function F in the PDE (1) is monotonically increasing with $F' \geq \nu_{\min} > 0$, then the operator $\mathcal{L} = \nu \partial^2 / \partial x^2$ on $\tilde{\mathbb{X}}$ subject to (15b)–(15c) and for L -periodic solutions has N zero eigenvalues and all other eigenvalues are negative and bounded away from zero by $\lambda \leq -\nu_{\min} \pi^2 / H^2$.*

Proof. The precisely N zero eigenvalues are established in the two paragraphs preceding the lemma. Lemma 2 establishes all eigenvalues of \mathcal{L} are real. Let λ be a non-zero eigenvalue and $v(x)$ be a corresponding eigenfunction. Then $v \perp \mathbb{E}$ by self-adjointness of \mathcal{L} , and, as usual,

$$(-\lambda)\|v\|^2 = -\lambda \langle v, v \rangle = \langle v, -\lambda v \rangle = \langle v, -\mathcal{L}v \rangle.$$

Decompose the eigenfunction into $v(x) = \tilde{v}(x) + \check{v}(x)$ where $\check{v}(x)$ is piecewise linear, continuous, and satisfies $\check{v}(X_j) = v(X_j)$, so that \tilde{v} is also continuous and $\tilde{v}(X_j) = 0$. Since $\check{v} \in \mathbb{E}$, so $\mathcal{L}\check{v} = 0$ (the check accent on \check{v} is to remind us of its piecewise linear nature). Consequently,

$$\begin{aligned} -\lambda\|v\|^2 &= \langle v, -\mathcal{L}v \rangle = \langle \tilde{v} + \check{v}, -\mathcal{L}\tilde{v} \rangle \\ &= \langle \tilde{v}, -\mathcal{L}\tilde{v} \rangle + \langle \check{v}, -\mathcal{L}\tilde{v} \rangle \\ &= \langle \tilde{v}, -\mathcal{L}\tilde{v} \rangle \end{aligned}$$

as, by self-adjointness, $\langle \check{v}, -\mathcal{L}\tilde{v} \rangle = \langle \mathcal{L}\check{v}, -\tilde{v} \rangle = \langle 0, -\tilde{v} \rangle = 0$. Thus, we proceed to derive the inequality

$$\begin{aligned} -\lambda\|v\|^2 &= \langle \tilde{v}, -\mathcal{L}\tilde{v} \rangle = \int_{\tilde{\mathbb{X}}} -\nu\tilde{v}\tilde{v}_{xx} dx \\ &= \sum_j [-\nu\tilde{v}\tilde{v}_x]_{X_{j-1}^+}^{X_j^-} + \int_{\tilde{\mathbb{X}}} \nu\tilde{v}_x^2 dx \quad (\text{integrating by parts}) \\ &= \sum_j 0 + \int_{\tilde{\mathbb{X}}} \nu\tilde{v}_x^2 dx \quad (\text{using } \tilde{v}(X_j^-) = \tilde{v}(X_j^+) = 0) \\ &\geq \nu_{\min} \int_{\tilde{\mathbb{X}}} \tilde{v}_x^2 dx \quad (\text{as } \nu(x) \geq \nu_{\min} > 0). \end{aligned}$$

The first consequence of this inequality is that there are no positive eigenvalues λ .

Secondly, relate this inequality to the spatially homogeneous problem. Let $\mathcal{L}_1 = \partial^2/\partial x^2$ denote the linear operator with coupling conditions appearing in (15) for the special case of $\nu(x) = \nu_j = 1$ for all x and j . Then, by the reverse argument to that of the previous paragraph,

$$\int_{\tilde{\mathbb{X}}} \tilde{v}_x^2 dx = \dots = \langle \tilde{v}, -\mathcal{L}_1\tilde{v} \rangle = \dots = \langle v, -\mathcal{L}_1v \rangle.$$

But, by the Rayleigh–Ritz theorem, the smallest magnitude, non-zero, eigenvalue λ_1 of \mathcal{L}_1 satisfies $-\lambda_1 = \min_{w \perp \mathbb{E}} \langle w, -\mathcal{L}_1w \rangle / \|w\|^2$, and so $\langle v, -\mathcal{L}_1v \rangle \geq -\lambda_1\|v\|^2$. Hence the inequalities give $-\lambda\|v\|^2 \geq \nu_{\min}(-\lambda_1)\|v\|^2$. By the next Lemma 4, $-\lambda_1 \geq \pi^2/H^2$, and so all eigenvalues satisfy $-\lambda \geq \nu_{\min}\pi^2/H^2$ as required. \square

Lemma 4 (spatially homogeneous spectrum). *The non-zero eigenvalues of the differential operator $\partial^2/\partial x^2$ on $\tilde{\mathbb{X}}$ with coupling conditions (15b)–(15c) when $\nu_j = 1$ all satisfy $\lambda \leq -\pi^2/H^2$.*

Proof. For the spatially homogeneous problem (15), set $\nu(x) = \nu_j = 1$. Seeking solutions $e^{\lambda t}v(x)$ leads to the ODE $\lambda v = v''$ on $\tilde{\mathbb{X}}$. As a constant coefficient ODE, and for eigenvalues $\lambda = -\kappa^2/H^2$ for some nondimensional wavenumber $\kappa \geq 0$ to be determined, its general solutions are of the form $v_j = A_j \cos \kappa \xi_j + B_j \sin \kappa \xi_j$ for coefficients A_j and B_j determined by the coupling conditions (15b)–(15c). Consequently, the spatial derivative is $v_{jx} = -\frac{A_j \kappa}{H} \sin \kappa \xi_j + \frac{B_j \kappa}{H} \cos \kappa \xi_j$.

Let's consider the spatial map $(A_j, B_j) \mapsto (A_{j+1}, B_{j+1})$. Continuity (15b) at $x = X_j$ ($\xi_j = 1$) requires

$$A_{j+1} = A_j \cos \kappa + B_j \sin \kappa = cA_j + sB_j,$$

where, for brevity in this proof, let $c := \cos \kappa$ and $s := \sin \kappa$. The derivative jump (15c) at $x = X_j$ requires

$$\frac{\kappa}{H}B_{j+1} + A_j \frac{\kappa}{H}s - B_j \frac{\kappa}{H}c = \frac{C(\gamma)}{H} [cA_{j+1} + sB_{j+1} - 2A_{j+1} + A_j],$$

where we include the factor $C(\gamma)$ for a little more generality; that is,

$$(c - 2)CA_{j+1} + (Cs - \kappa)B_{j+1} + (C - s\kappa)A_j + c\kappa B_j = 0.$$

Dividing by C and setting $\kappa' = \kappa/C$ gives the equivalent

$$(c - 2)A_{j+1} + (s - \kappa')B_{j+1} + (1 - s\kappa')A_j + c\kappa' B_j = 0.$$

Considering together the two mapping equations, this spatial map has solutions $(A_j, B_j) \propto \mu^j$ for some multiplier μ only for vanishing determinant

$$\det \begin{bmatrix} \mu - c & -s \\ \mu(c - 2) + 1 - s\kappa' & \mu(s - \kappa') + c\kappa' \end{bmatrix} = 0;$$

that is, $\mu^2 - 2\frac{s - c\kappa'}{s - \kappa'}\mu + 1 = 0.$ (16)

Hence the two possible multipliers of the spatial map are

$$\mu = \beta \pm \sqrt{\beta^2 - 1} \quad \text{for } \beta = \frac{s - c\kappa'}{s - \kappa'}.$$

Consequently, $|\beta| > 1$ is not possible as then there would be two (real) multipliers: one with magnitude greater than one, representing structures growing exponentially quickly to the right; and one with magnitude less than one, representing structures growing exponentially quickly to the left. The only allowable cases occur for $|\beta| \leq 1$ when the multipliers are complex

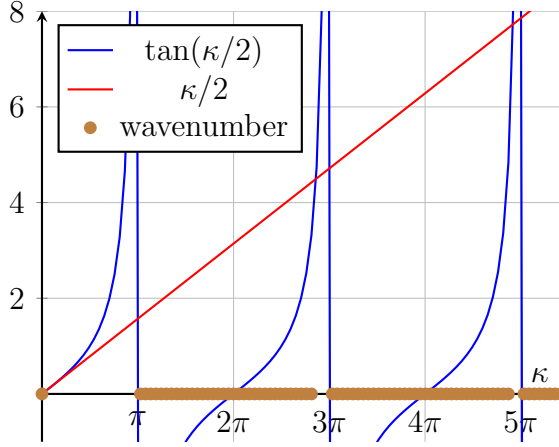


Figure 5: The linearised ($\gamma = 0$, $C = 1$) spectrum determined by the spectral requirement (17). The thick lines along the κ -axis indicate regions of spatial wavenumbers for which the corresponding spatial structures are bounded for all space.

of magnitude $|\mu| = 1$, and so characterise periodic structures in space. Since $\kappa' - s = \kappa/C(\gamma) - \sin \kappa \geq 0$, the requirement $|\beta| \leq 1$ becomes $s - \kappa' \leq c\kappa' - s \leq \kappa' - s$; that is, $2s - \kappa' \leq c\kappa' \leq \kappa'$. The right-hand inequality is always satisfied as $c = \cos \kappa$, but the left-hand inequality requires $2s \leq (1 + c)\kappa'$, that is, $s/(1 + c) \leq \kappa'/2$. Recalling $s = \sin \kappa$ and $c = \cos \kappa$, this requirement becomes

$$\tan \frac{\kappa}{2} \leq \frac{\kappa}{2C}. \quad (17)$$

As illustrated by Figure 5, for the specific case of the linearised problem (15) for which $C(0) = 1$, the smallest allowable nonzero nondimensional wavenumber is $\kappa = \pi$. Hence the smallest magnitude nonzero eigenvalue is $\leq -\pi^2/H^2$ as required. \square

The reason to include $C(\gamma)$ in the proof is to comment on the linearisation about another subspace of equilibria. As well as the piecewise linear equilibria \mathbb{E} at $\gamma = \alpha = 0$, another subspace of equilibria are $u = \text{constant}$ on \mathbb{X} for nonlinearity $\alpha = 0$ but now for arbitrary coupling parameter γ . The linearisation about this set of equilibria is also the system (15) but with $\nu(x) = F'(0)$, constant, and with factor $1/H$ in the coupling (15c) replaced by $C(\gamma)/H$. The proof of Lemma 4 also applies to this case. Inequality (17) then gives allowed wavenumbers for general γ . As coupling parameter γ varies from zero to one, the factor $C(\gamma)$ varies from one to zero, and so the denominator C in inequality (17) increases the slope of the straight line of Figure 5. Thus the set of allowed wavenumbers increases with coupling γ , and, in particular, the gap $(0, \pi)$ between the slow and the fast modes fills up with the slow modes. It is in this manner that the continuum of allowed wavenumbers is restored in the fully coupled PDE over the whole domain \mathbb{X} .

Theorem 5 (slow manifold). *Consider the nonlinear PDE (1) on domain $\tilde{\mathbb{X}}$ with coupling conditions (12) and preconditions as recorded earlier.*

1. *In an open domain \mathcal{E} containing the subspace \mathbb{E} there exists a slow manifold,*

$$u = u(x, \vec{U}, \gamma, \alpha) \quad \text{such that} \quad \frac{d\vec{U}}{dt} = \vec{g}(\vec{U}, \gamma, \alpha). \quad (18)$$

2. *This slow manifold is emergent in the sense that for all solutions $u(x, t)$ of (1)+(12), that stay in \mathcal{E} , there exists a solution $\vec{U}(t)$ of (18) such that $u(x, t) = u(x, \vec{U}(t), \gamma, \alpha) + \mathcal{O}(e^{-\mu t})$ for decay rate $\mu \approx \nu_{\min} \pi^2 / H^2$.*
3. *Given two smooth functions $\tilde{u}(x, \vec{U}, \gamma, \alpha)$ and $\tilde{g}(\vec{U}, \gamma, \alpha)$ for the governing equations (1)+(12), evaluated at $u = \tilde{u}$ such that $d\vec{U}/dt = \tilde{g}$, having residuals $\mathcal{O}(\gamma^p + \alpha^q)$ as $(\gamma, \alpha) \rightarrow \vec{0}$, then the slow manifold is*

$$u = \tilde{u}(x, \vec{U}, \gamma, \alpha) + \mathcal{O}(\gamma^p + \alpha^q) \quad \text{such that} \quad \frac{d\vec{U}}{dt} = \tilde{g}(\vec{U}, \gamma, \alpha) + \mathcal{O}(\gamma^p + \alpha^q).$$

Proof. The preconditions for the centre manifold theorems of Haragus & Iooss (2011) [Chapter 2] hold. We consider smooth, L -periodic, square integrable functions on $\tilde{\mathbb{X}}$ where ‘smooth’ means continuously differentiable as often as necessary, which forms the requisite Hilbert spaces. The self-adjoint, linearised operator (15) of diffusion on a finite spatial domain forms an analytic semigroup (Haragus & Iooss 2011, Remark 2.18, e.g.), and the functions F and G of the PDE (1) are assumed smooth to thus satisfy Hypothesis 2.1 and 2.7 of Haragus & Iooss (2011). Lemma 3, under the proviso that $F' \geq \nu_{\min} > 0$, establishes the Spectral Decomposition Hypothesis 2.4 of Haragus & Iooss (2011).

1. Theorem 2.9 of Haragus & Iooss (2011) then establishes that for each point of \mathbb{E} (parametrised by \vec{U}) a *local centre manifold* $\mathcal{M}_{\vec{U}}$ exists in some neighbourhood $\mathcal{E}_{\vec{U}}$ in the $(\vec{U}, \gamma, \alpha)$ -space. Because the centre eigenvalues are all zero (Lemma 3), they are more precisely called *local slow manifolds*. Setting $\mathcal{M} := \bigcup_{\vec{U}} \mathcal{M}_{\vec{U}}$ and domain $\mathcal{E} := \bigcup_{\vec{U}} \mathcal{E}_{\vec{U}}$ the slow manifold \mathcal{M} exists in the domain \mathcal{E} (containing \mathbb{E}) as required.



2. The unstable spectrum is empty (Lemma 3), so Theorem 3.22 of Haragus & Iooss (2011) applies to establish the exponentially quick emergence of the slow manifold to all solutions that remain within \mathcal{E} for all

time. The rate of attraction to the slow manifold in \mathcal{E} is estimated by the linearised rate at \mathbb{E} by continuity in perturbations (Roberts 2014, §11.3, e.g.).

3. Under corresponding preconditions, Proposition 3.6 of Potzsche & Rasmussen (2006) proves that if an approximation to the slow manifold (18) gives residuals of the system's equations which are zero to some order, then the slow manifold is approximated to the same order of error. Here introduce parameter ϵ and set $\gamma = c\epsilon^q$ and $\alpha = a\epsilon^p$. Then regard quantities as a Taylor series in ϵ with coefficients parametrised by (\vec{U}, c, a) . Also, the process $\epsilon \rightarrow 0$ implies $(\gamma, \alpha) \rightarrow \vec{0}$. By supposition, the given \tilde{u} and \tilde{g} have residuals $\mathcal{O}(\gamma^p + \alpha^q) = \mathcal{O}(c^p \epsilon^{pq} + a^q \epsilon^{pq}) = \mathcal{O}(\epsilon^{pq})$ as $\epsilon \rightarrow 0$. By Proposition 3.6 of Potzsche & Rasmussen (2006), \tilde{u} and \tilde{g} approximate the slow manifold to errors $\mathcal{O}(\epsilon^{pq})$, and hence the errors are $\mathcal{O}(\gamma^p + \alpha^q)$.

The more wide ranging theorems of Aulbach & Wanner (1996, 1999, 2000) could also be invoked to establish this theorem. \square

The evolution equation (18), $d\vec{U}/dt = g(\vec{U}, \gamma, \alpha)$, is the in-principle exact closure for a discretisation of the dynamics of the nonlinear PDE (1).

4 Nonlinear modelling of Burger's PDE

This section uses Burgers' PDE (2) as an example of the construction of a slow manifold discrete model. Burgers' PDE (2) is in the class (1) addressed by the theory of Section 3 and so Theorem 5 assures us a slow manifold model exists.

Proposition 3.6 by Potzsche & Rasmussen (2006) underlies the construction as it asserts the order of error of an approximation is the same as the order of error of the residuals of the governing equations. Given the existence of a slow manifold $u = u(x, \vec{U})$ such that $\dot{\vec{U}} = \vec{g}(\vec{U})$, and implicitly a function of coupling γ and nonlinearity α , we rewrite Burgers' PDE (2) in the form

$$\mathcal{R}(u, \vec{g}) = 0 \quad \text{with residual } \mathcal{R}(u, \vec{g}) := -\frac{\partial u}{\partial \vec{U}} \cdot \vec{g} + \nu \frac{\partial^2 u}{\partial x^2} - \alpha u u_x. \quad (19)$$

The initial approximation to the slow manifold is, in terms of the local space variable $\xi_j = (x - X_{j-1})/H$ defined by (13), the piecewise linear field

$$u^0 = \sum_{j=1}^N \chi_j(x) [(1 - \xi_j)U_{j-1} + \xi_j U_j] \quad \text{where } \chi_j(x) = \begin{cases} 1 & \text{if } x \in \mathbb{X}_j, \\ 0 & \text{if } x \notin \mathbb{X}_j. \end{cases} \quad (20)$$

We seek the slow manifold for the coupled and nonlinear dynamics in a multi-variate power series in corresponding parameters γ and α . But to simplify the algebraic construction process we follow the approach of Jarrad (2001) and introduce one ordering parameter $\varepsilon = \sqrt{\gamma^2 + \alpha^2}$ and label terms depending upon their order in ε . For example, a term in $\gamma^p \alpha^q$ is termed of order ε^{p+q} . Then we seek expressions for the slow manifold in the asymptotic series

$$u(x, \vec{U}, \gamma, \alpha) \sim \sum_{n=0}^{\infty} u^n(x, \vec{U}, \gamma, \alpha), \quad \vec{g}(\vec{U}, \gamma, \alpha) \sim \sum_{n=1}^{\infty} \vec{g}^n(\vec{U}, \gamma, \alpha), \quad (21)$$

where u^n and \vec{g}^n are of order n in the order parameter ε . The partial sums of these series are

$$u^{(n)}(x, \vec{U}, \gamma, \alpha) := \sum_{p=0}^n u^p, \quad \vec{g}^{(n)}(\vec{U}, \gamma, \alpha) := \sum_{p=1}^n \vec{g}^p. \quad (22)$$

Then $u = u^{(n)} + \mathcal{O}(\varepsilon^{n+1})$ and $u^{(n)} = u^{(n-1)} + u^n$; likewise for $\vec{g}^{(n)}$ and \vec{g}^n . Substituting these into the governing PDE (19) and rearranging we deduce


$$\mathcal{R}(u^{(n)}, \vec{g}^{(n)}) = -\frac{\partial u^0}{\partial \vec{U}} \cdot \vec{g}^n + \nu \frac{\partial^2 u^n}{\partial x^2} + \mathcal{R}(u^{(n-1)}, \vec{g}^{(n-1)}) + \mathcal{O}(\varepsilon^{n+1}).$$

Hence to require $\mathcal{R}(u^{(n)}, \vec{g}^{(n)}) = \mathcal{O}(\varepsilon^{n+1})$, the process is to iteratively solve

$$\nu \frac{\partial^2 u^n}{\partial x^2} = \frac{\partial u^0}{\partial \vec{U}} \cdot \vec{g}^n - \mathcal{R}(u^{(n-1)}, \vec{g}^{(n-1)}). \quad (23)$$

First order approximation Obtain the first approximation by solving (23) for the case $n = 1$ given the initial subspace approximation (20). Equation (23) becomes

$$\nu \frac{\partial^2 u^1}{\partial x^2} = \sum_{j=1}^N \chi_j(x) \left\{ [\xi_j + (1 - \xi_j)\sigma^{-1}] g_j^1 + \alpha ([\xi_j + (1 - \xi_j)\sigma^{-1}] U_j) \frac{1}{H} \nabla U_j \right\},$$

for backward difference $\nabla = 1 - \sigma^{-1}$.  Spatially integrating twice gives

$$\begin{aligned} \nu u^1 = & \sum_{j=1}^N \chi_j(x) \left\{ d_j + H \xi_j c_j + \frac{H^2}{6} [\xi_j^3 + (1 - \xi_j)^3 \sigma^{-1}] g_j^1 \right. \\ & \left. + \frac{\alpha H}{6} ([\xi_j^3 + (1 - \xi_j)^3 \sigma^{-1}] U_j) \nabla U_j \right\}. \end{aligned}$$

- The interelement continuity condition (12a) requires that $u^n(X_j, \vec{U}) = 0$ for $n = 1, 2, 3, \dots$, because $u^0(X_j, \vec{U}) = U_j = u(X_j, \vec{U})$. Hence, we solve for d_j at $\xi_j = 0$ and c_j at $\xi_j = 1$, giving

$$\begin{aligned}
\nu u^1 &= \sum_{j=1}^N \chi_j(x) \left\{ \frac{H^2}{6} [\xi_j^3 + (1 - \xi_j)^3 \sigma^{-1} - \xi_j \nabla - \sigma^{-1}] g_j^1 \right. \\
&\quad \left. + \frac{\alpha H}{6} ([\xi_j^3 + (1 - \xi_j)^3 \sigma^{-1} - \xi_j \nabla - \sigma^{-1}] U_j) \nabla U_j \right\} \\
&= \sum_{j=1}^N \chi_j(x) \left\{ \frac{H^2}{6} \mathcal{I}_1 g_j^1 + \frac{\alpha H}{6} (\mathcal{I}_1 U_j) \nabla U_j \right\}, \tag{24}
\end{aligned}$$

where it is convenient to introduce interpolation operators $\mathcal{I}_0(\xi_j) := \xi_j + (1 - \xi_j)\sigma^{-1}$ and $\mathcal{I}_1(\xi_j) := \xi_j^3 + (1 - \xi_j)^3 \sigma^{-1} - \xi_j \nabla - \sigma^{-1}$ (observe that $\mathcal{I}_1'' = 6\mathcal{I}_0/H^2$).

- The interelement smoothness condition (12b) determines the value of g_j^1 . Substitute u^1 from (24) into (12b) and we require

$$-\frac{\nu\gamma}{H} \delta^2 U_j = -H \left(1 + \frac{1}{6} \delta^2 \right) g_j^1 - \frac{\alpha}{3} (U_j \mu \delta U_j + \mu \delta U_j^2).$$

For this to be satisfied we set

$$g_j^1 = S \left[\frac{\nu\gamma}{H^2} \delta^2 U_j - \frac{\alpha}{3H} U_j \mu \delta U_j - \frac{\alpha}{3H} \mu \delta U_j^2 \right],$$

where operator $S := (1 + \delta^2/6)^{-1}$.

Combining these with the initial approximation gives the slow manifold

$$u = \sum_{j=1}^N \chi_j(x) \left\{ \mathcal{I}_0 U_j + \frac{H^2}{6\nu} \mathcal{I}_1 g_j^1 + \frac{\alpha H}{6\nu} \mathcal{I}_1 U_j \nabla U_j \right\} + \mathcal{O}(\varepsilon^2), \tag{25a}$$

$$\dot{U}_j = S \left[\frac{\nu\gamma}{H^2} \delta^2 U_j - \frac{\alpha}{3H} U_j \mu \delta U_j - \frac{\alpha}{3H} \mu \delta U_j^2 \right] + \mathcal{O}(\varepsilon^2). \tag{25b}$$

Apart from the nonlocal operator S , this discrete closure (25b) is just the mixture model (5) with $\theta = \frac{2}{3}$. This parameter value is exactly the critical value predicted by Fornberg (1973) to be necessary for the stability of numerical integration of the mixture model with $\nu = 0$ and $\alpha = 1$.

Connection to a cubic spline An intriguing property of the operator $S = (1 + \delta^2/6)^{-1} = 6(\sigma + 4 + \sigma^{-1})^{-1}$ is that it is precisely the operator found in constructing a cubic spline interpolation through equi-spaced data. For example, if the general cubic spline for the j th interval is specified as $S_j(x) = a_j H^3 \xi_j^3/6 + b_j H^2 \xi_j^2/2 + c_j H \xi_j + d_j$, then its second derivative at the left-hand end of the interval is given by $b_j = S\delta^2 d_j/H^2$, and the corresponding first and third derivatives by $c_j = \nabla \sigma d_j/H - H(2 + \sigma)b_j/6$ and $a_j = \nabla \sigma b_j/H$, respectively (Burden & Faires 1985, e.g.). As $d_j = U_{j-1}$ in our example, comparison with the first-order approximation derived above reveals that the holistic approach ensures a cubic spline formulation when $\alpha = 0$ and $\gamma = 1$.

Higher order approximations Higher order terms in the asymptotic series for u may be systematically computed by iteratively solving equation (23) after having first computed \bar{g}^n . The solvability condition determines the latter (Jarrad 2001), namely that the right-hand side of equation (23) must be orthogonal to the null-space of the adjoint of $\nu \partial^2/\partial x^2$. Since the operator is self-adjoint, we isolate the boundary between the j th and $(j+1)$ th intervals with the triangular finite-element

$$\hat{v}_0 = \chi_j(x)\xi_j + \chi_{j+1}(x)(1 - \xi_j), \quad (26)$$

which satisfies both the continuity condition (12a) and the smoothness condition (12b) (for $\gamma = 0$). Now, recalling that $u^n(X_j, \vec{U}) = 0$ for $n \geq 1$, and hence $[\nu u_x^n]_j = 0$ for $n \geq 2$, taking the inner product of equation (23) with \hat{v}_0 gives rise to the solvability condition

$$HS^{-1}g_j^n - \langle \mathcal{R}(u^{(n-1)}, \bar{g}^{(n-1)}), \hat{v}_0 \rangle = 0 \text{ for } n = 2, 3, \dots \quad (27)$$

The higher order advection terms in α and the interactions between α and γ rapidly become more complex. For example, the $\gamma\alpha$ terms are

$$\begin{aligned} g_j^2 = & \frac{1}{H} \left\{ -\frac{1}{10} S(U_j S \mu \delta U_j) - \frac{1}{6} S(U_j \mu \delta U_j) + \frac{1}{10} S(SU_j \mu \delta U_j) \right. \\ & - \frac{1}{5} S^2(U_j S \mu \delta U_j) + \frac{13}{30} S^2(U_j \mu \delta U_j) - \frac{1}{15} S^3(U_j \mu \delta U_j) \\ & - \frac{1}{15} S^3 \mu \delta U_j^2 + \frac{7}{30} S^2 \mu \delta U_j^2 + \frac{2}{5} U_j S \mu \delta U_j - \frac{11}{30} S \mu \delta U_j^2 \Big\} \\ & + \mathcal{O}(\gamma^2, \alpha^2). \end{aligned} \quad (28)$$

In contrast, the terms purely in the homotopy parameter γ represent smoothing corrections to the diffusion; for example, the coarse dynamics of the dif-

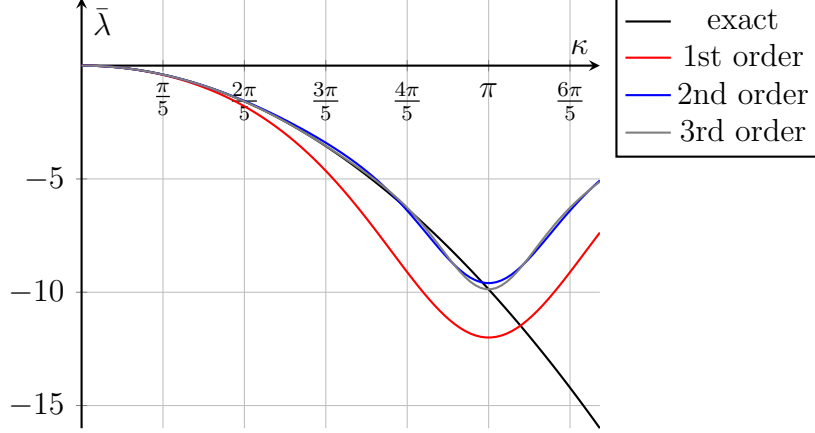


Figure 6: The non-dimensionalised spectrum ($\bar{\lambda} = \lambda H^2/\nu$ versus $\kappa = kH$) of the diffusion equation ($\alpha = 0$) for the mode $\tilde{u}(x, t) = e^{\lambda t + i k x}$, contrasting the continuum dynamics against successive discrete, holistic approximations (for $\gamma = 1$).

fusion equation ($\alpha = 0$) obey

$$\begin{aligned} \dot{U}_j = & \frac{\nu\gamma}{H^2} S \delta^2 U_j + \frac{\nu\gamma^2}{60H^2} (7 - 2S) S^2 \delta^4 U_j \\ & + \frac{\nu\gamma^3}{6300H^2} (94 - 73S + 14S^2) S^3 \delta^6 U_j + \mathcal{O}(\gamma^4). \end{aligned} \quad (29)$$

Figure 6 shows that each additional term in this expansion provides a better approximation to the full continuum dynamics.

5 Dynamical stability of the discretisation

To investigate the theoretical stability of discrete approximations to Burgers' equation (2), we consider a mostly undisturbed system where $U_j = 0$ at all grid-points except for M adjacent, internal points. For example, for $M = 2$ it suffices to choose $N = M + 1 = 3$ intervals with outer points fixed at $U_0 = U_N = 0$. Hence, with the transformation $U_j = \frac{\nu}{\alpha H} V_j$, the mixture model (5) reduces to

$$\begin{aligned} \frac{H^2}{\nu} \dot{V}_1 &= -2V_1 + V_2 - \frac{(1-\theta)}{2} V_1 V_2 - \frac{\theta}{4} V_2^2, \\ \frac{H^2}{\nu} \dot{V}_2 &= V_1 - 2V_2 + \frac{(1-\theta)}{2} V_1 V_2 + \frac{\theta}{4} V_1^2. \end{aligned}$$

This reduced system has a stable critical point at $V_1 = V_2 = 0$ with non-dimensionalised eigenvalues $\bar{\lambda} = \frac{H^2}{\nu}\lambda = -1, -3$, and an unstable critical point at $V_1 = -V_2 = \frac{12}{2-3\theta}$ with eigenvalues $\bar{\lambda} = \frac{2}{2-3\theta} \pm \frac{|4-9\theta|}{|2-3\theta|}$. Observe that the unstable point is removed to infinity when $\theta = \frac{2}{3}$. This is exactly the critical value predicted by Fornberg (1973) to be necessary (but not always sufficient) for numerical stability of the mixture model with $\nu = 0, \alpha = 1$. Consequently, the corresponding reduction of the holistic model (6), namely

$$\begin{aligned}\frac{H^2}{\nu}\dot{V}_1 &= -4V_1 + \frac{11}{4}V_2 - \frac{1}{12}V_1^2 - \frac{3}{8}V_1V_2 - \frac{7}{24}V_2^2, \\ \frac{H^2}{\nu}\dot{V}_2 &= \frac{11}{4}V_1 - 4V_2 + \frac{7}{24}V_1^2 + \frac{3}{8}V_1V_2 + \frac{1}{12}V_2^2,\end{aligned}$$

is unconditionally stable with critical point at $V_1 = V_2 = 0$ and eigenvalues $\bar{\lambda} = -\frac{5}{4}, -\frac{27}{4}$.

Similarly, for $M = 3$ consecutive points the mixture model (5) reduces to

$$\begin{aligned}\frac{H^2}{\nu}\dot{V}_1 &= -2V_1 + V_2 - \frac{(1-\theta)}{2}V_1V_2 - \frac{\theta}{4}V_2^2, \\ \frac{H^2}{\nu}\dot{V}_2 &= V_1 - 2V_2 + V_3 - \frac{(1-\theta)}{2}V_2(V_3 - V_1) - \frac{\theta}{4}(V_3^2 - V_1^2), \\ \frac{H^2}{\nu}\dot{V}_3 &= V_2 - 2V_3 + \frac{(1-\theta)}{2}V_2V_3 + \frac{\theta}{4}V_2^2.\end{aligned}$$

Substitution of $V_1 = aV_2$ and $V_3 = bV_2$ then leads to

$$V_1 = \frac{\mu(4 - \mu\theta)}{8 + 2\mu(1 - \theta)}, \quad V_2 = \mu, \quad V_3 = \frac{\mu(4 + \mu\theta)}{8 - 2\mu(1 - \theta)},$$

where μ satisfies

$$\mu[\theta(1 - \theta)(\theta^2 - 3\theta + 1)\mu^4 + 16(2\theta^2 - 4\theta + 1)\mu^2 - 256] = 0. \quad (30)$$

Observe that the coefficient of μ^4 vanishes at $\theta = 0, 1$ and $\theta_c = \frac{3-\sqrt{5}}{2}$. It can then be shown that the trivial critical point (for $\mu = 0$) is unconditionally stable, and that a pair of unstable, nontrivial critical points occur when $0 < \theta < \theta_c$. Note that the holistic parameter value of $\theta = \frac{2}{3}$ lies in the range $\theta_c \leq \theta \leq 1$ for which there are no nontrivial critical points. Interestingly, the purely advective form ($\theta = 0$) is now also unconditionally stable for $M = 3$.

Turning now to numerical simulation, we assume a 2π -periodic domain with $\nu = 1$ and $\alpha = 1$ for convenience. The initial field $u(x, 0) = A \sin x$ is integrated at the $N + 1$ grid-points $X_j = Hj$, $j = 0, 1, \dots, N$, with spacing $H = \frac{2\pi}{N}$. The integration is performed for a maximum duration of $T = 10$, but

ceases early at the first sign of an instability, being either: a magnitude $|U_j|$ exceeding 1000 (denoted by 'x'); or an non-monotonic irregularity (denoted by '+'). The smallest value of A for which an instability occurs is plotted against a selection of values for the number N of discretised intervals, as shown in Figures 7–8.

Observe that for $N = 3$ intervals, only the advective model ($\theta = 0$) displays an instability corresponding to the unstable critical point deduced above for $M = 2$. Additionally, numerical instability does not occur for the advective model for $N = 4$, corresponding to the lack of unstable critical points deduced above for $M = 3$. Overall, the onset of instability for the advective model occurs at lower amplitudes than for the other models, which agrees with empirical observations (Fornberg 1973, e.g.).

6 Conclusion

??

Acknowledgements AJR thanks the ARC for partial support of this project through grant DP150102385.

References

- Aulbach, B. & Wanner, T. (1996), Integral manifolds for Caratheodory type differential equations in Banach spaces, *in* B. Aulbach & F. Colonius, eds, ‘Six Lectures on Dynamical Systems’, World Scientific, Singapore, pp. 45–119.
- Aulbach, B. & Wanner, T. (1999), Invariant foliations for Caratheodory type differential equations in Banach spaces, *in* V. Lakshmikantham & A. A. Martynyuk, eds, ‘Advances of Stability Theory at the End of XX Century’, Gordon & Breach Publishers. <http://citeseerx.ist.psu.edu/viewdoc/download?doi=10.1.1.45.5229&rep=rep1&type=pdf>.
- Aulbach, B. & Wanner, T. (2000), ‘The Hartman–Grobman theorem for Caratheodory-type differential equations in Banach spaces’, *Nonlinear Analysis* **40**, 91–104. doi:10.1016/S0362-546X(00)85006-3.
- Burden, R. L. & Faires, J. D. (1985), *Numerical Analysis (third edition)*, Prindle, Weber and Schmidt.

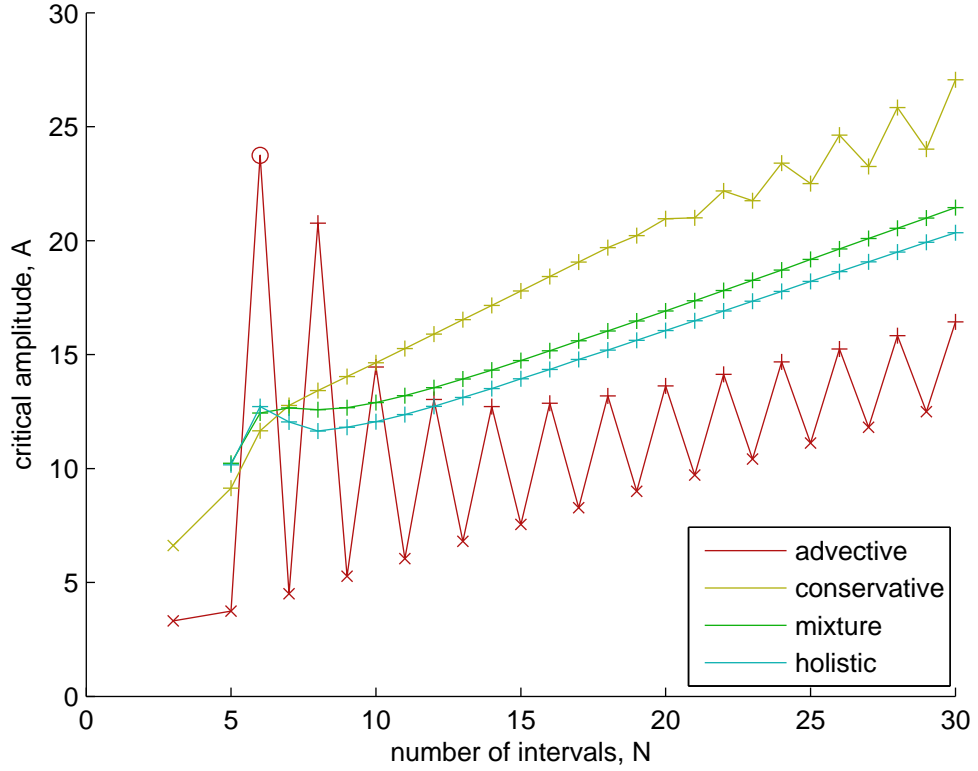


Figure 7: Stability of numerical integration of Burgers' PDE, starting from $u(x, 0) = A \sin x$. The holistic model is contrasted with the general mixture model for $\theta = 0$ (advective), $\theta = 1$ (conservative) and $\theta = \frac{2}{3}$ (mixture). Instability is detected either when $|U_j| > 1000$ (denoted by 'x'), or by the occurrence of non-monotonic modes (denoted by '+'). The plots show the smallest values of A for which instability occurs in the various models for each value of N .

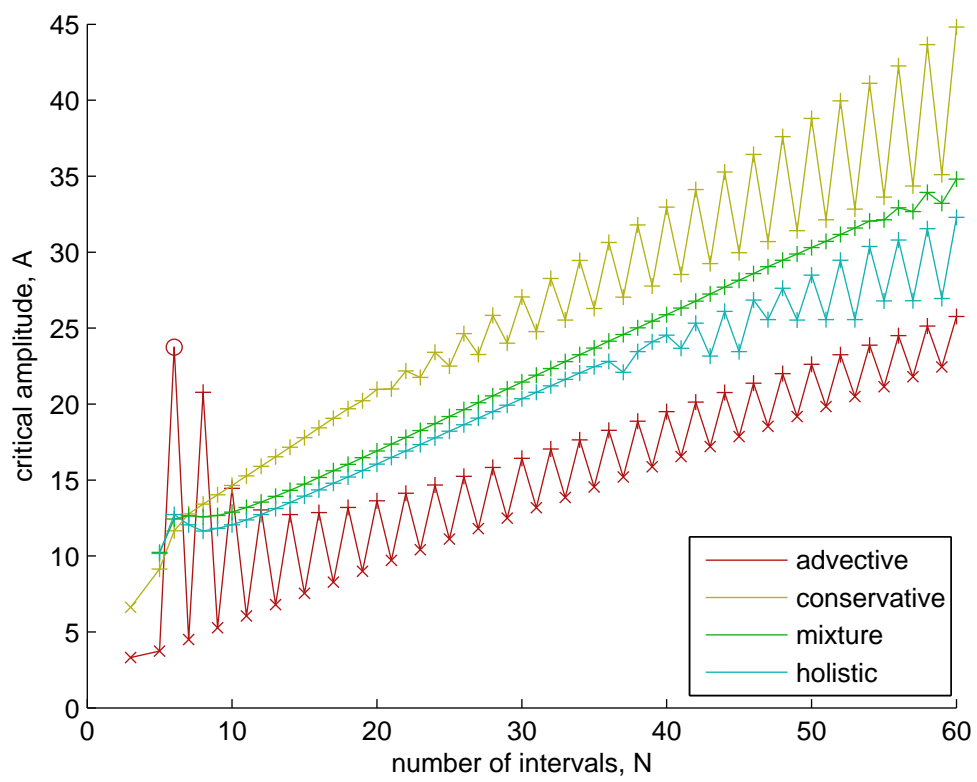


Figure 8: Hmm?

- Carr, J. (1981), *Applications of centre manifold theory*, Vol. 35 of *Applied Math. Sci.*, Springer-Verlag.
<http://books.google.com.au/books?id=93BdN7btysoc>
- Fornberg, B. (1973), ‘On the instability of the leap-frog and Crank–Nicolson approximations of a nonlinear partial differential equation’, *Maths of Comput.* **27**, 45–57.
- Haragus, M. & Iooss, G. (2011), *Local Bifurcations, Center Manifolds, and Normal Forms in Infinite-Dimensional Dynamical Systems*, Springer.
doi:10.1007/978-0-85729-112-7.
- Jarrad, G. A. (2001), *Perturbations, Chaos and Waves*, PhD thesis, University of South Australia.
- Mercer, G. N. & Roberts, A. J. (1990), ‘A centre manifold description of contaminant dispersion in channels with varying flow properties’, *SIAM J. Appl. Math.* **50**, 1547–1565. <http://link.aip.org/link/?SMM/50/1547/1>.
- O’Leary, D. P. (2008), *Scientific Computing with Case Studies*, SIAM, Philadelphia.
<http://www.ec-securehost.com/SIAM/OT109.html>
- Potzsche, C. & Rasmussen, M. (2006), ‘Taylor approximation of integral manifolds’, *Journal of Dynamics and Differential Equations* **18**, 427–460.
<http://dx.doi.org/10.1007/s10884-006-9011-8>
- Roberts, A. J. (1997), ‘Low-dimensional modelling of dynamics via computer algebra’, *Computer Phys. Comm.* **100**, 215–230. doi:10.1016/S0010-4655(96)00162-2.
- Roberts, A. J. (2001), ‘Holistic discretisation ensures fidelity to Burgers’ equation’, *Applied Numerical Modelling* **37**, 371–396. doi:10.1016/S0168-9274(00)00053-2.
<http://arXiv.org/abs/chao-dyn/9901011>
- Roberts, A. J. (2003), ‘A holistic finite difference approach models linear dynamics consistently’, *Mathematics of Computation* **72**, 247–262.
<http://www.ams.org/mcom/2003-72-241/S0025-5718-02-01448-5>
- Roberts, A. J. (2014), *Model emergent dynamics in complex systems*, SIAM, Philadelphia.
<http://bookstore.siam.org/mm20/>

Roberts, A. J., MacKenzie, T. & Bunder, J. (2014), ‘A dynamical systems approach to simulating macroscale spatial dynamics in multiple dimensions’, *J. Engineering Mathematics* **86**(1), 175–207.
<http://arxiv.org/abs/1103.1187>

Strang, G. & Fix, G. (2008), *An Analysis of the Finite Element Method*, 2nd edn, SIAM, Philadelphia.
<http://bookstore.siam.org/wc08/>

A Ancillary material: computer algebra ...

```

1  %% Key:
2  %% hh := H = X_j - X_{j-1}
3  %% xi := xi_j = (x - X_{j-1}) / H
4  %% uu = U_j
5  %% p := E^+ = sigma, right-shift
6  %% m := E^- = sigma^{-1}, left-shift
7  %% d2 := delta^2 = p + m - 2
8  %% ss := S = (1 + delta^2/6)^{-1}
9  %% md := mu*delta = (p - m)/2
10
11 on div; off allfac; on revpri;
12 factor hh, alpha, gamma, nu;
13
14 depend xi, j;
15 depend uu, j, t;
16 depend gg, j;
17
18 operator p, m, d2, md, ss;
19 linear p, m, d2, md, ss;
20
21 %% Expansions
22 let p(~z,j) => z + md(z,j) + d2(z,j)/2,
23     m(~z,j) => z - md(z,j) + d2(z,j)/2;
24
25 %% Independence
26 let md(1,j) => 0,
27     d2(1,j) => 0,
28     ss(1,j) => 1;
29
```

```

30 %% Canonical orderings
31 let md(ss(~z,j),j) => ss(md(z,j),j);
32 let d2(ss(~z,j),j) => ss(d2(z,j),j);
33 let md(d2(~z,j),j) => d2(md(z,j),j);
34
35 %% Invariants:
36 % Next follows from direct expansion, and is required for  $p(m(z)) = m(p(z)) =$ 
37 let md(md(~z,j),j) => d2(z,j) + d2(d2(z,j),j)/4;
38 % Next follows from definition of S:
39 let ss(d2(~z,j),j) => 6*(z-ss(z,j));
40 % Next follows from expanding  $\mu \cdot \delta z^2$ :
41 let d2(~y,j)*md(~z,j) => md(z^2,j) - 2*z*md(z,j) when y=z;
42 % Next two follow from  $p(y*m(z)) = p(y)*z$  and  $m(y*p(z)) = m(y)*z$ :
43 let md(~y*md(~z,j),j) => 1/2*(1/2*d2(y*d2(z,j),j) + y*d2(z,j) - z*d2(y,j) + d
44 let md(~y*d2(~z,j),j) => d2(y*md(z,j),j) + 2*(y*md(z,j) + z*md(y,j) - md(y*z,
45 % Next follows from either  $m(z)^2 = m(z^2)$  or  $p(z)^2 = p(z^2)$ :
46 let md(~z,j)^2 => 1/2*d2(z^2,j) - 1/4*d2(z,j)^2 - z*d2(z,j);
47
48 % Temporo-spatial composition:
49 let df(uu,t) => gg;
50 operator !~f;
51 let df(~f(~z,j),t) => f(df(z,t),j);
52 let df(~z,x) => df(z,xi)/hh;
53 let df(~z,x,2) => df(z,xi,2)/hh^2;
54
55 % Initiate approximations:
56 u0 := xi*uu + (1-xi)*m(uu,j);
57 u := u0;
58 g := 0;
59
60 let gamma^2 => 0, alpha^2 => 0;
61 for iter := 1:3 do begin
62
63 % Check internal boundary conditions:
64 amp := sub(xi=1,u) - uu; % u|X_j = U_j
65 cty := sub(xi=0,p(u,j)) - sub(xi=1,u); % [u]_j = 0
66 ux := df(u,x)$
67 jmp := sub(xi=0,p(ux,j)) - sub(xi=1,ux)
68 - (1-gamma)*sub(xi=1,d2(u,j))/hh; % [u']_j = (1-gamma)/H*delta^2 U_j
69 pde := -sub(gg=g,df(u,t)) + nu*df(ux,x) - alpha*u*ux;
70

```

```

71 % Satisfy solvability condition,  $\langle v_0, pde \rangle = 0$ , where  $v_0 := xi + p(1-xi, j)$ , to
72 % ensure internal boundary conditions are met.
73 % (Note: Use temporary variables to avoid weird error in integration):
74 pde_xi := pde*xi$
75 pde_1mxi := (1-xi)*pde$
76 slv := (int(pde_xi, xi, 0, 1) + p(int(pde_1mxi, xi, 0, 1), j))*hh + nu*jmp;
77 % Update g from error in solvability:
78 gn := ss(slv, j)/hh;
79 % Update u by solving pde = 0 for u := u + u_n:
80 tn := xi*gn + (1-xi)*m(gn, j) - pde$
81 un := hh^2*int(int(tn, xi), xi)/nu$
82 % Impose integration constants to satisfy  $u_n|_{X_{j-1}} = 0$ ,  $u_n|_{X_j} = 0$ :
83 un := un - sub(xi=1, un)*xi;
84 % Update iteration:
85 u := u + un;
86 g := g + gn;
87
88 end;
89
90 % Check internal boundary conditions:
91 amp := sub(xi=1, u) - uu; %  $u|_{X_j} = U_j$ 
92 cty := sub(xi=0, p(u, j)) - sub(xi=1, u); %  $[u]_j = 0$ 
93 ux := df(u, x)$
94 jmp := sub(xi=0, p(ux, j)) - sub(xi=1, ux)
95         - (1-gamma)*sub(xi=1, d2(u, j))/hh; %  $[u']_j = (1-\gamma)/H\delta^2 U_j$ 
96 pde := -sub(gg=g, df(u, t)) + nu*df(ux, x) - alpha*u*ux;
97
98 % Apply further invariants for advection terms:
99 let ss(md(ss(uu, j)*uu, j), j) =>
100     ss(ss(md(uu, j), j)*uu, j)
101     - 1/2*ss(md(uu, j)*ss(uu, j), j)
102     - 3/2*ss(md(uu, j), j)*uu
103     + 3/2*ss(md(uu^2, j), j);
104
105 let ss(md(uu, j)*ss(md(uu, j), j), j) =>
106     18*uu**2
107     - 9*ss(uu, j)*uu
108     + 6*ss(ss(uu, j)*uu, j)
109     - 3/2*ss(d2(uu, j)*uu, j)
110     - 2*ss(md(ss(md(uu, j), j)*uu, j), j)
111     - 15*ss(uu**2, j);

```

```

112
113 let ss(d2(uu,j)*ss(md(uu,j),j),j) =>
114   - 6*ss(md(uu,j)*uu,j)
115   + 3*ss(md(uu,j)*ss(uu,j),j)
116   - 3*ss(md(uu,j),j)*uu
117   + 3*ss(md(uu**2,j),j);
118
119 let ss(md(ss(md(uu,j),j)*uu,j),j) =>
120   - 6*ss(uu,j)*uu
121   + 3*ss(ss(uu,j)*uu,j)
122   - 1/2*ss(d2(uu,j)*ss(uu,j),j)
123   - 6*ss(uu**2,j)
124   + 9*uu**2;
125
126 end;

```